A peer-reviewed open-access journal
NeoBiota
Advancing research on alien species and biological invasions

NeoBiota 110: 21–41 (2026)
DOI: 10.3897/neobiota.110.208923

Research Article

Metagenomic and amplicon sequencing uncover adaptation and sympatric coexistence of the alien snail *Rumina decollata* (Linnaeus, 1758) (Stylommatophora, Achatinidae) with native terrestrial snails in East China

Yang Xu[1*], Ming Gao[1*], Gaoji Zhang[1], Yingzhu Li[1], Hongyi Liu[1]

1 *College of Life Sciences, Nanjing Forestry University, Nanjing, 210037, China*
Corresponding author: Hongyi Liu (hongyi_liu@njfu.edu.cn)

Abstract

Alien species expand beyond their native ranges by withstanding ecological stress and exploiting diverse resources, yet the potential contribution of the microbiome to ecological persistence in novel environments remains poorly understood. The Mediterranean snail *Rumina decollata* is classified as invasive in numerous foreign regions while being merely regarded as an alien species in China, where it coexists sympatrically with native *Acusta ravida* and *Euphaedusa aculus* snails across eastern China. Gut microbial samples of *R. decollata* were collected from urban residential quarters, a university campus, and a mountain park in Nanjing for metagenomic sequencing, and 16S rRNA and ITS amplicon sequencing were conducted on the three snail species and surrounding soils. Conserved microbial pathways suggest broad metabolic potential for diverse dietary resources. Chitin related pathways were enriched in mountain populations, while xenobiotic degradation pathways were more represented in urban individuals, indicating habitat associated functional variation. Amplicon data demonstrated that gut microbiota were distinctly separated from soil communities, indicating clear host-associated differentiation. The gut microbiome of *R. decollata* was more similar to that of *A. ravida*, potentially reflecting similarities in plant resource use. Collectively, host-associated gut microbiota differentiation and habitat-dependent functional variation are consistent with potential ecological differentiation and provide insights into the microbiome associated with the coexistence of these snail species.

Key words: Ecological adaptation, functional plasticity, gut microbiome, resource utilization

OPEN ACCESS

Academic editor: Jianghua Sun
Received: 23 July 2026
Accepted: 16 October 2026
Published: 27 October 2026

Citation: Xu Y, Gao M, Zhang G, Li Y, Liu H (2026) Metagenomic and amplicon sequencing uncover adaptation and sympatric coexistence of the alien snail *Rumina decollata* (Linnaeus, 1758) (Stylommatophora, Achatinidae) with native terrestrial snails in East China. NeoBiota 110: 21–41. https://doi.org/10.3897/neobiota.110.208923

Copyright: © Yang Xu et al.
This is an open access article distributed under terms of the Creative Commons Attribution License (Attribution 4.0 International – CC BY 4.0).

Introduction

Globalization has accelerated the movement of organisms beyond their native ranges, making biological invasions a major challenge in contemporary ecology. Although many introduced species fail to establish persistent populations, others successfully survive and expand in novel environments, eventually becoming invasive. Understanding why some alien species can overcome environmental constraints and persist outside their native ranges remains a fundamental question in invasion biology (Blackburn et al. 2011; Richardson and Pyšek 2012). Successful establishment requires introduced organisms to cope with unfamiliar abiotic conditions,

* These authors contributed equally to this work.

acquire suitable resources, and interact with resident communities. However, the mechanisms underlying such ecological flexibility remain poorly understood.

Environmental heterogeneity represents an important selective force shaping species adaptation. Habitats differing in resource availability, vegetation structure, soil properties, and anthropogenic disturbance impose distinct ecological pressures that influence resource utilization and species interactions (McGill et al. 2006; Vellend 2010). For alien species, the ability to adjust to heterogeneous environments may determine whether introduced populations remain localized or achieve long-term persistence. Identifying ecological processes associated with early establishment is therefore important for understanding invasion potential.

Terrestrial snails provide an ideal but understudied system for investigating these processes because of their limited mobility, strong dependence on soil and vegetation, and flexible dietary strategies (Santamaria et al. 2023). *Rumina decollata* (Linnaeus, 1758), (Stylommatophora, Achatinidae), native to the Mediterranean region, has expanded its distribution to North and South America, Africa, and Asia through human-mediated introduction, and is considered invasive in several introduced regions due to its establishment success and potential impacts on native snails (Cowie 2001; Pizá et al. 2023). However, populations in eastern China are currently regarded as alien populations rather than formally recognized invasive populations. Despite its successful establishment across diverse habitats, the mechanisms supporting its persistence and coexistence with native snails remain unknown.

The gut microbiome can influence host physiology, resource utilization, and responses to environmental variation. Microbial symbionts may expand host metabolic capacity, facilitate the utilization of novel resources, degrade complex substrates, and enhance stress tolerance (McFall-Ngai et al. 2013; Douglas 2015). For alien species, gut microbiomes may provide a rapid-response component of adjustment to new environments without requiring immediate host evolutionary changes. Although microbiome-mediated effects on host environmental have been demonstrated in insects and aquatic invertebrates, their ecological significance in terrestrial snails remain poorly understood. (Yun et al. 2014; Pierce and Ward 2019).

Current gastropod microbiome studies have mainly focused on bacterial communities and a limited number of species, such as the invasive Giant African Snail, *Achatina fulica* (Férussac, 1821) (Cardoso et al. 2012; Pawar et al. 2012). While metagenomic approaches have revealed functional potentials, targeted investigation of gut fungal communities and their ecological contributions to host adaptation remains largely unexplored in terrestrial snails. Moreover, anthropogenic environments may expose alien species to microbial risk factors, including antibiotic resistance genes (ARGs) and virulence-associated traits, as already evidenced in invasive snails (Cardoso et al. 2012). Environmental microbial communities affected by human activities can serve as reservoirs of resistance determinants, and animal-associated microbiomes may represent potential interfaces linking environmental microbes, hosts, and pathogens (Martínez 2008; Forsberg et al. 2012; Zhu et al. 2013).

A central question in alien species ecology is what extent associated microbiomes reflect environmental microbial exposure versus host-associated processes during microbiome assembly. Terrestrial snails continuously interact with soil, vegetation, and sympatric organisms, providing opportunities for microbial exchange. Host-associated processes may nevertheless contribute to the establishment and maintenance of distinct gut microbial communities despite environmental expo-

sure (Ley et al. 2008; Colston and Jackson 2016). Resolving the balance between environmental exposure and host-associated processes is essential for understanding microbiome-mediated adaptation.

Here, we investigated the gut microbiome of the alien snail *R. decollata* across heterogeneous habitats in Nanjing, China, and compared it with two sympatric native snails (*Acusta ravida* (Benson, 1842) (Stylommatophora, Camaenidae) and *Euphaedusa aculus* (Benson, 1842) (Stylommatophora, Clausiliidae)) and surrounding soil microbiota. By integrating metagenomic sequencing with bacterial (16S rRNA gene) and fungal (ITS) amplicon sequencing, we examined habitat-associated functional variation, host-associated microbial assembly, and the potential ecological relevance of microbiome organization to ecological adaptation and coexistence of this alien snail. We further evaluated ARGs and virulence-associated functions to assess potential ecological and public health implications.

Materials and methods

Collecting and processing samples

Three different habitats were selected in Nanjing, China; namely Pailou Lane (PL, 32°2'38.455620"N, 118°46'19.630272"E), Nanjing Forestry University (NF, 32°4'48.758520"N, 118°49'5.664324"E), and Fangshan Park (FS, 31°54'8.683920"N, 118°52'21.664812"E). Twelve individuals of *R. decollata* were collected from each habitat. All snails were starved for 48 h to allow gut evacuation and maintained individually in sterile containers during starvation to minimize cross-contamination, after which the midgut and hindgut were dissected under sterile conditions. Due to the low biomass of individual gut tissues, the midgut and hindgut from two individuals collected from the same habitat were pooled into one biological replicate prior to DNA extraction. Thus, each pooled biological replicate represented two individuals. Six pooled biological replicates were generated for each habitat, yielding a total of 18 pooled biological replicates for metagenomic sequencing.

Additionally, 15 *R. decollata* and two native snail species (*A. ravida*, n = 10; *E. aculus*, n = 10) were collected from a sympatric habitat at the Nanjing Forestry University campus. In this habitat, the environmental soil was collected from three 15 m × 15 m sampling plots using the 5-point sampling method, and the three samples were homogenized using a 2 mm sieve. These three snail species were also starved for 48 h and then dissected under sterile conditions to obtain the same intestinal regions. The collected intestinal tissues and soil samples were all stored in sterile cryogenic tubes and immediately frozen in liquid nitrogen and stored at -80 °C until DNA extraction. DNA extracted from these sympatrically collected gut and soil samples was used for 16S rRNA gene and ITS region amplicon sequencing.

DNA extraction

Genomic DNA was extracted from the gut of all snail specimens using the cetyltrimethylammonium bromide (CTAB) method (Winnepenninckx et al. 1993; Kwong et al. 2017). Soil DNA was extracted from 0.5 g of homogenized soil using the TIANamp Soil DNA Kit (centrifugal column format, catalog no. DP336, TianGen Biotech, Beijing, China) following the manufacturer's instructions.

Metagenomic analysis

Library construction and sequencing

DNA concentration was measured using a Qubit fluorometer, and DNA integrity was assessed by agarose gel electrophoresis. Only intact, non-degraded DNA samples with sufficient yield (≥1 μg) were used (Lee et al. 2012; Nakayama et al. 2016). For each sample, 1 μg of qualified genomic DNA was fragmented to an average size of 350 bp using a Covaris ultrasonic disruptor. Paired-end libraries were prepared via end repair, A-tailing, adapter ligation, size selection, purification, and PCR amplification. Library quality was assessed on a Fragment Analyzer (Agilent, USA), and effective library concentrations (≥3 nM) were quantified by quantitative PCR. Libraries were sequenced on the Illumina NovaSeq 6000 platform with paired-end 150-bp reads, yielding approximately 10 Gb of raw data per sample (Quail et al. 2012; Quince et al. 2017).

Raw data preprocessing and host removal

Raw reads were quality-filtered using fastp (v0.23.2) to remove adapter-contaminated, low-quality (Q ≤ 5 bases >50%) and N-rich (ambiguous bases >10%) reads (Chen et al. 2018). Host-derived reads were then filtered by aligning clean reads against the available chromosome-level genome of *A. fulica* using Bowtie2 (v2.4.5) (Langmead and Salzberg 2012). Because a high-quality reference genome for *R. decollata* is not publicly available, the *A. fulica* genome was used as a surrogate host reference (Guo et al. 2019). Alignments with mismatches and multi-mapped reads were discarded. Given the phylogenetic distance between *R. decollata* and the surrogate *A. fulica* reference, this alignment-based host removal was only partially effective. We therefore performed direct gene annotation against a target-taxon-specific reference database to maximize the removal of residual host-derived sequences.

Assembly and non-redundant gene catalog

Clean reads after initial host-read filtering were assembled using MEGAHIT (v1.2.9), and scaffolds ≥500 bp were retained (Li et al. 2015). Open reading frames (ORFs) were predicted from the retained scaffolds using MetaGeneMark (v3.38), and ORFs ≥100 nt were retained. The predicted ORFs were clustered using CD-HIT (v4.8.1) with a sequence identity threshold of 95% and a minimum alignment coverage of 90% to generate an initial non-redundant gene catalog (Zhu et al. 2010; Fu et al. 2012). Non-host reads from each sample were mapped back to the gene catalog using Bowtie2 (v2.4.5) to estimate gene abundance. Genes supported by ≤2 mapped reads were discarded to remove extremely low-abundance sequences (Forslund et al. 2015).

Gene abundance was calculated from the number of mapped reads and gene length. The mapped read count of each gene was divided by its gene length to obtain a length-corrected abundance, which was then normalized against the mean length-corrected abundance of all genes in the corresponding sample. The resulting normalized gene abundance values were used for downstream functional analyses.

Taxonomic annotation

Taxonomic annotation of the non-redundant gene catalog was performed using DIAMOND (v2.1.9) against the Micro_NR database, which was constructed from the NCBI non-redundant (NR) protein database and included Bacteria, Fungi, Archaea, and Viruses (Buchfink et al. 2021; Wang et al. 2024). DIAMOND searches were conducted using an e-value threshold of 1e–5, a maximum of 50 target hits per query, a minimum sequence identity of 30%, and the sensitive search mode. Taxonomic assignments were determined using the lowest common ancestor (LCA) approach based on the resulting homologous protein matches (Huson et al. 2016; Buchfink et al. 2021). This taxonomic annotation step also served as a second-stage host filtering procedure to remove residual host-derived sequences not eliminated by initial reference mapping. Genes assigned to microbial taxa were retained for subsequent functional annotation and analysis (Wang et al. 2017).

Functional annotation

Functional annotation was performed against the Kyoto Encyclopedia of Genes and Genomes (KEGG v2024.03), Carbohydrate-Active enZYmes (CAZy v2024.03), and Virulence Factor Database (VFDB v2024.06) databases using DIAMOND (v2.1.9) (Kanehisa and Goto 2000; Lombard et al. 2014; Buchfink et al. 2015; Liu et al. 2019). The same DIAMOND search parameters described above were used for functional annotation. For each unigene, the highest-scoring hit was retained for functional assignment. Functional annotations were summarized according to the classification systems of the respective databases, and the relative abundance of each functional category was calculated by summing the relative abundances of genes assigned to that category. For CAZy, annotations were summarized at the CAZy family level, and the relative abundance of each CAZy family was calculated by summing the relative abundances of genes assigned to that family. Antibiotic resistance genes (ARGs) were identified using the Resistance Gene Identifier (RGI v6.0.2) against the Comprehensive Antibiotic Resistance Database (CARD v3.2.6) using default parameters (Alcock et al. 2020).

16S and ITS gene amplicon sequencing

The bacterial and fungal communities were characterized by amplicon sequencing of the 16S rRNA gene and the internal transcribed spacer (ITS) region. The V3–V4 region of the bacterial 16S rRNA gene was amplified using the primer pair 341F (5'-CCTAYGGGRBGCASCAG-3') /806R (5'-GGACTACNNGGGTATCTAAT-3'), and the fungal ITS1-5F region was amplified using the primer pair ITS5 (5'-GGAAGTAAAAGTCGTAACAAGG-3') /ITS2-2043R (5'-GCTGCGTTCTTCATCGATGC-3') (Caporaso et al. 2011; Herlemann et al. 2011; Toju et al. 2012). PCR products were purified, quantified, pooled at equimolar concentrations, and sequenced on an Illumina NovaSeq 6000 platform using paired-end 250 bp chemistry.

Raw sequencing reads were demultiplexed according to barcode sequences, merged using FLASH, quality-filtered with fastp, and processed in QIIME2 (v2022.02) (Magoč and Salzberg 2011; Chen et al. 2018; Bolyen et al. 2019).

Amplicon sequence variants (ASVs) were inferred using the DADA2 algorithm following chimera removal. Taxonomic assignment was performed against the SILVA ribosomal RNA gene database (SILVA) (v138.2) for bacterial 16S sequences and the UNITE fungal ITS database (UNITE) (v10.0) for fungal ITS sequences (Quast et al. 2013; Callahan et al. 2016; Nilsson et al. 2019). All 38 DNA samples were subjected to 16S rRNA gene amplification and sequencing. For the ITS region, two samples consistently failed to yield PCR products and were therefore excluded. A total of 36 samples were retained for fungal community analyses.

Statistical analysis

Functional profiles of KEGG, CAZy, VFDB, and CARD annotations were compared among habitats using Bray-Curtis-based non-metric multidimensional scaling (NMDS), analysis of similarities (ANOSIM; 999 permutations), and linear discriminant analysis effect size (LEfSe; LDA > 3.5). Pairwise ANOSIM comparisons were further performed to evaluate differences between individual habitat pairs. Microbial alpha diversity (Chao1 and Shannon indices) was compared using the Kruskal-Wallis test. Differences in the relative abundances of microbial taxa among groups were assessed using the Kruskal-Wallis test. Beta diversity was evaluated using weighted UniFrac and Bray-Curtis distances and visualized by principal coordinate analysis (PCoA) and NMDS. Differences in microbial community composition were assessed using permutational multivariate analysis of variance (PERMANOVA; 999 permutations), and shared and differentially abundant taxa were identified using Venn diagrams and LEfSe (LDA > 3.5). Cross-domain bacterial-fungal association networks were constructed separately for the integrated and *R. decollata* datasets based on Spearman's rank correlations. For each sample, paired bacterial and fungal ASV tables were used to construct cross-domain co-occurrence networks, ensuring that correlations reflect within-sample associations. Only robust and statistically significant correlations satisfying dataset-specific filtering criteria were retained for network construction. Procrustes analysis was performed using the same paired datasets. Network topological properties were calculated using the igraph package and visualized in Gephi (v0.11.2). Concordance between bacterial and fungal community structures was evaluated using Procrustes analysis based on Bray-Curtis distance matrices (999 permutations). Unless otherwise specified, statistical analyses were performed in R (v4.2.0) using the vegan, igraph, ggplot2, and related packages, with statistical significance defined as $P < 0.05$.

Results

Functional profiles of gut microbiomes of Rumina decollata across different habitats

Metagenomic sequencing overview

High-quality metagenomic sequencing was successfully performed for all 18 pooled biological replicates. After quality filtering, each pooled biological replicate yielded 9.62–15.55 Gb of clean data, with Q30 values ranging from 98.16% to 98.72% and GC contents from 39.40% to 40.94% (Suppl. material 1: table S1). Total assembly sizes ranged from 803.19 to 904.79 Mb, with N50 values between 2,587 and 6,236 bp. To minimize the influence of residual host-derived sequences,

the gene catalog was refined by retaining only genes assigned to microbial taxa (Suppl. material 1: table S2).

Functional variation of gut microbiomes across different habitats

KEGG Level 2 annotations revealed broadly similar functional compositions among habitats, although notable shifts in the relative abundance of specific metabolic categories were evident (Fig. 1a). NMDS based on KEGG level 3 annotations visualized separation in functional profiles among three habitats, with partial overlap among groups (stress = 0.02; Fig. 1b). ANOSIM detected a significant difference in overall functional profiles among habitats (R = 0.20, P = 0.006). Pairwise ANOSIM comparisons further revealed significant differences between FS and NF (R = 0.3222, P = 0.006) and between FS and PL (R = 0.1444, P = 0.045), whereas the difference between NF and PL was not significant (R = 0.1778, P = 0.070). The heatmap further illustrated differences in the abundance patterns of KEGG level 3 pathways across habitats (Fig. 1c), and the corresponding pathway classifications are provided in Suppl. material 1: table S3.

CAZy family composition was broadly similar among habitats, although differences in the relative abundance of several enzyme families were observed (Fig. 1d; Suppl. material 1: table S4). NMDS based on CAZy family profiles showed substantial overlap among habitats (stress = 0.03; Fig. 1e), and ANOSIM detected no significant difference among habitats (R = 0.10, P = 0.065).

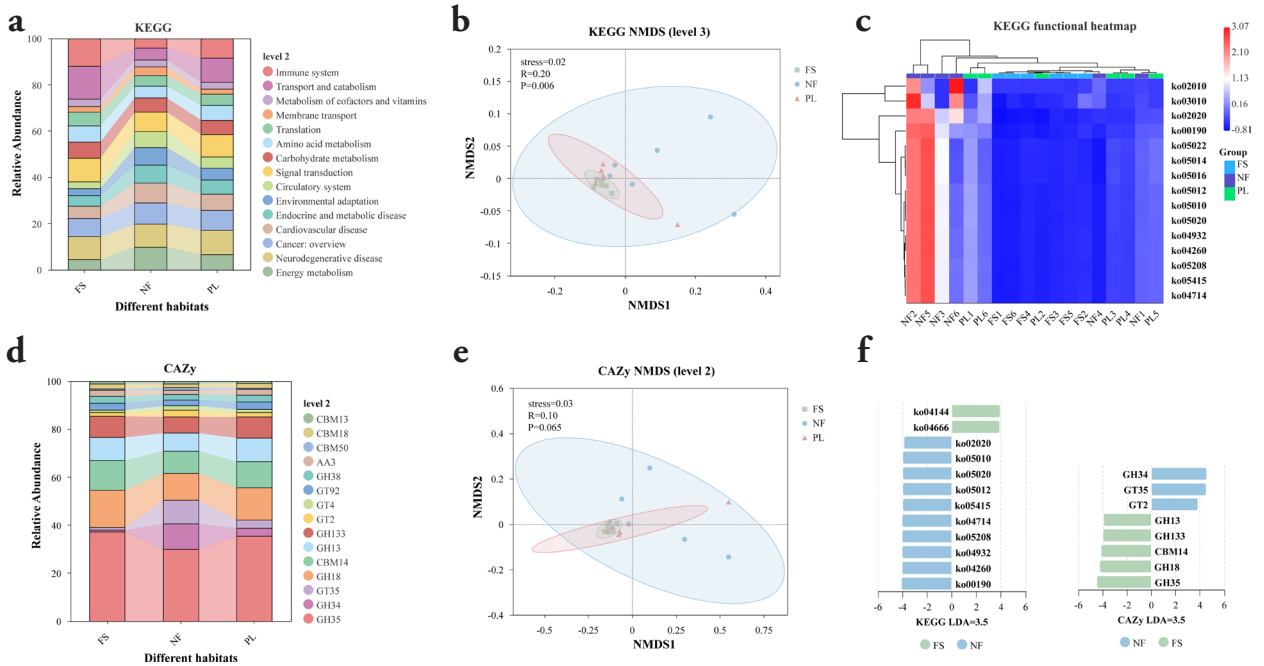

Figure 1. Functional variation of the gut microbiome of *Rumina decollata* across different habitats. **a.** Relative abundance of Kyoto Encyclopedia of Genes and Genomes (KEGG) Level 2 functional categories in gut microbiomes from different habitats; **b.** Non-metric multidimensional scaling (NMDS) based on KEGG Level 3 annotations showing differences in functional profiles among habitats. Ellipses represent 95% confidence intervals; **c.** Heatmap showing the relative abundance patterns of the most abundant KEGG level 3 pathways across samples; **d.** Relative abundance of Carbohydrate-Active enZYmes (CAZy) family categories across the three habitats; **e.** NMDS ordination based on CAZy family profiles. Ellipses represent 95% confidence intervals; **f.** LEfSe analysis (LDA > 3.5) identifying KEGG level 3 pathways and CAZy families significantly enriched in different habitat groups. No significant biomarkers were detected in the PL group. FS, NF and PL represent the three habitats described in the Materials and Methods.

LEfSe analysis (LDA > 3.5) identified differentially abundant functional features among habitats (Fig. 1f). For KEGG, ko04144 (Endocytosis) and ko04666 (Fc gamma R-mediated phagocytosis) were enriched in the FS group, whereas ko02020, ko05010, ko05020, ko05012, ko05415, ko04714, ko05208, ko04932, ko04260, and ko00190 were significantly enriched in the NF group (Suppl. material 1: table S5). In the CAZy dataset, the GH34 and GT35 families were enriched in the NF group, while GH13, GH133, CBM14, GH18, and GH35 were enriched in the FS habitats (Suppl. material 1: table S6). Moreover, the relative abundance of chitinase (GH18) was 5.72% in FS, compared with 4.74% in NF, and 5.32% in PL; chitin-binding module (CBM14) was 5.34% in FS, 4.43% in NF, and 4.96% in PL. Meanwhile, relative abundance of the xenobiotic metabolism pathway ko00362 (benzoate degradation) was 0.0375% in NF, 0.0092% in FS, and 0.0158% in PL, with NF having the highest level.

Virulence factor and antibiotic resistance profiles across different habitats

At the VFDB level 2, virulence factor profiles were broadly similar among the three different habitats, although differences in the relative abundance of several virulence categories were observed (Fig. 2a; Suppl. material 1: table S7). NMDS based on VFDB annotations showed substantial overlap among habitat groups (stress = 0.05; Fig. 2b). ANOSIM detected no significant difference in virulence profiles among habitats (R = 0.09, P = 0.098). LEfSe analysis (LDA > 3.5) identified several differentially abundant virulence associated categories, with Capsule,

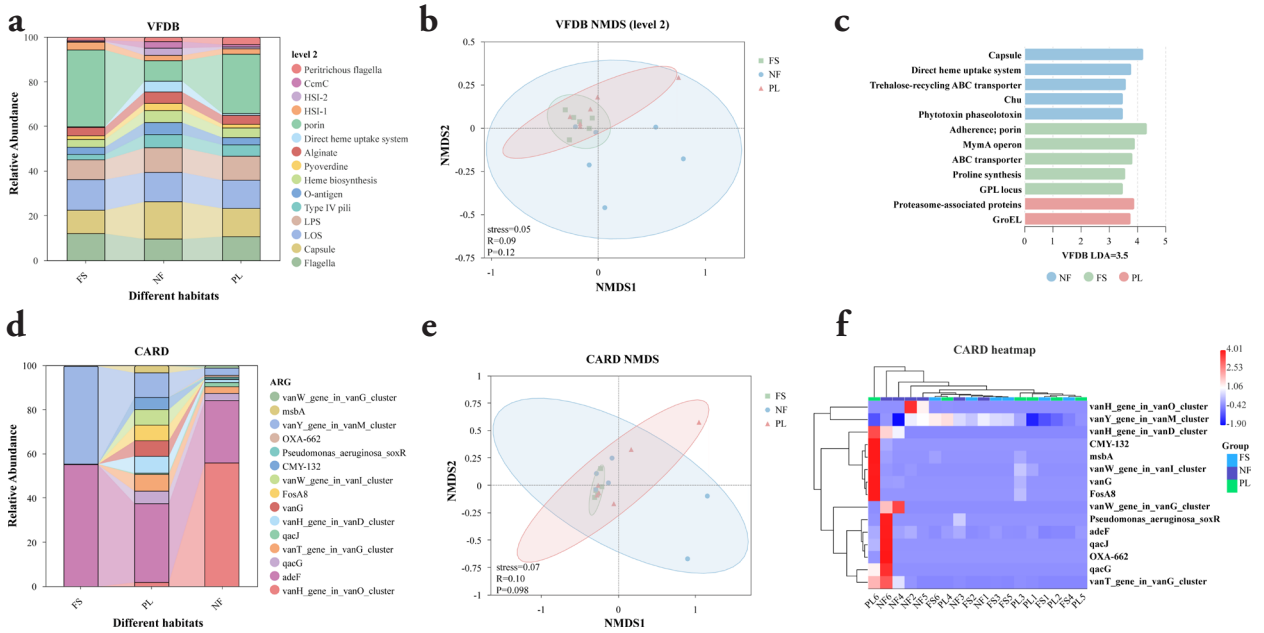

Figure 2. Virulence factor and antibiotic resistance profiles of the gut microbiome of *Rumina decollata* across different habitats. **a.** Relative abundance of Virulence Factor Database (VFDB) Level 2 virulence factor categories in gut microbiomes from different habitats (FS, NF, and PL); **b.** Non-metric multidimensional scaling (NMDS) based on VFDB Level 2 annotations showing differences in virulence factor profiles among habitats; **c.** LEfSe analysis (LDA > 3.5) identifying habitat-enriched virulence factor categories. No significant biomarkers were detected in the PL group; **d.** Relative abundance of antibiotic resistance gene (ARG) classes annotated against the CARD database across different habitats; **e.** NMDS based on CARD annotations showing similarities in ARG profiles among habitats; **f.** Heatmap showing the relative abundance patterns of ARG classes across samples.

Exoenzyme, and T6SS enriched in the NF group, whereas Type IV secretion system, Flagella, and Toxin were enriched in the FS group (Fig. 2c; Suppl. material 1: table S8).

CARD annotations showed broadly similar ARG compositions across habitats (Fig. 2d; Suppl. material 1: table S9). NMDS based on CARD annotations showed substantial overlap in ARG profiles among habitats (stress = 0.07; Fig. 2e), and ANOSIM did not detect significant differences in overall ARG profiles among habitats. The heatmap showed variation in the relative abundance of individual ARG classes across samples, with some ARG classes occurring at higher relative abundances in the NF group (Fig. 2f).

Bacterial community structure and diversity of three sympatric snail species and associated soil

16S rRNA sequencing data

A total of 3,815,224 high-quality sequences were obtained from the 38 samples, with an average read length of 415.46 bp. After quality filtering and denoising, 16,268 ASVs were identified. Taxonomic annotation assigned these ASVs to 2 domains (Bacteria and Archaea), 58 phyla, 139 classes, 322 orders, 569 families, 1,480 genera, and 1,913 species.

Three sympatric snail species and composition of soil bacterial communities

Bacterial community composition was characterized at the phylum and genus levels (Fig. 3a). Pseudomonadota and Bacillota were among the dominant phyla across all groups, with descriptive variation in their relative abundances among groups (P = 0.023 and 0.038, respectively). Bacillota predominated in soil and *A. ravida*, whereas Pseudomonadota was relatively more abundant in *A. ravida* and *R. decollata*. Cyanobacteriota exhibited a high proportion in *E. aculus*, while Actinomycetota presented significantly higher relative abundance in *R. decollata* compared with other groups.

At the genus level, the dominant genera of *R. decollata* were *Cutibacterium* (12.9%), *Corynebacterium* (12.3%), *Staphylococcus* (5.8%), *Enhydrobacter* (5.5%), and *Lactobacillus* (1.4%). *A. ravida* was dominated by *Mycoplasma* (14.4%), *Lactobacillus* (5.6%), and *Burkholderia-Caballeronia-Paraburkholderia* (4.0%). In the gut of *E. aculus*, *Lactobacillus* (3.2%) was the dominant genus, while *Cutibacterium* and *Staphylococcus* were also commonly present. In the sympatric soil where all three snails coexisted, the dominant genera were *Lactobacillus* (30.4%), *Ligilactobacillus* (6.4%), *Limosilactobacillus* (5.9%), and *Mediterraneibacter* (5.6%). Venn diagram analysis showed that all four groups shared 105 genera, whereas the numbers of unique genera were 303 in *R. decollata*, 292 in *A. ravida*, 42 in *E. aculus*, and 25 in soil (Fig. 3b).

Diversity and compositional differentiation of bacterial communities

Alpha diversity differed among groups (Fig. 3c). Chao1 richness was higher in *R. decollata* and soil than in the other groups, while *E. aculus* showed the lowest

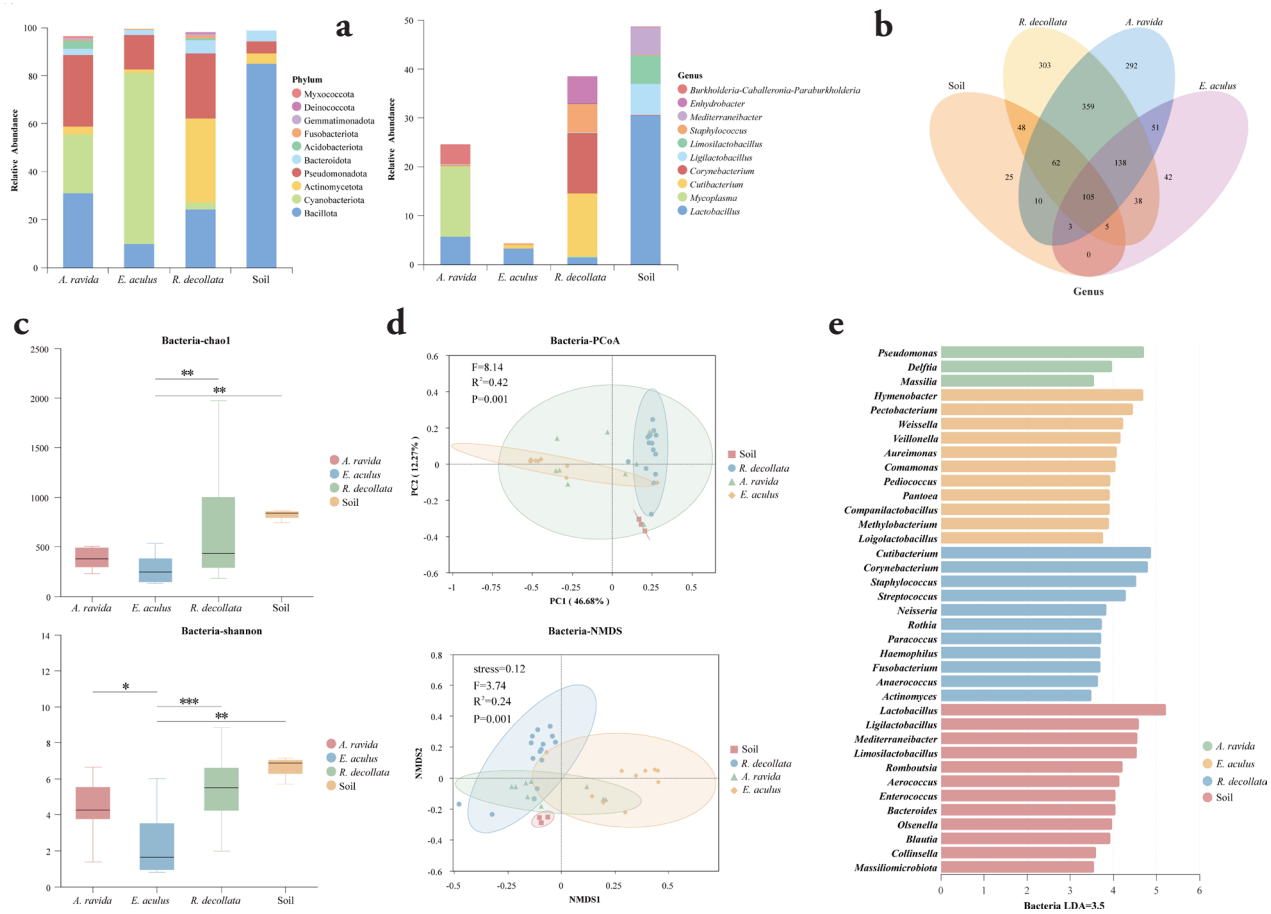

Figure 3. Bacterial community composition and diversity of three sympatric snail species and associated soil. **a.** Relative abundance of dominant bacterial taxa at the phylum (left) and genus (right) levels in the gut microbiota of *Rumina decollata*, *Acusta ravida*, *Euphaedusa aculus*, and sympatric soil; **b.** Venn diagram showing the numbers of shared and unique bacterial genera among the four groups; **c.** Alpha diversity of bacterial communities based on the Chao1 richness and Shannon diversity indices. $*p \leq 0.05$, $**p \leq 0.01$, $***p \leq 0.001$; **d.** Beta diversity of bacterial communities based on weighted UniFrac principal coordinate analysis (PCoA, upper side) and Bray-Curtis non-metric multidimensional scaling (NMDS, lower side); **e.** LEfSe analysis (LDA > 3.5) showing bacterial taxa significantly enriched in each group.

diversity (Shannon index, $P < 0.05$). *R. decollata* also exhibited higher inter-individual variation.

To examine differences in community composition, beta diversity was evaluated using weighted UniFrac and Bray-Curtis distance metrics. Principal coordinate analysis (PCoA) based on weighted UniFrac distances showed clear separation among soil, *R. decollata*, and the two other snail species (Fig. 3d). Consistent patterns were observed in non-metric multidimensional scaling (NMDS, stress = 0.12) ordination based on Bray-Curtis distances, with partial overlap between *A. ravida* and *R. decollata*. Permutational multivariate analysis of variance (PERMANOVA, $F = 8.14$, $R^2 = 0.42$, $P = 0.001$; 999 permutations) confirmed that group identity significantly explained variation in community composition.

LEfSe analysis (LDA > 3.5) identified group-specific bacterial biomarkers (Fig. 3e). *R. decollata* was enriched in *Cutibacterium*, *Corynebacterium*, and *Staphylococcus* (all LDA > 4.5). Soil was characterized by *Lactobacillus*, *Ligilactobacillus*, *Mediterraneibacter*, and *Limosilactobacillus*, while *A. ravida* and *E. aculus* were enriched in *Pseudomonas* and *Hymenobacter*.

Fungal community structure and diversity in three sympatric snail species and soil

ITS sequencing data

A total of 3,577,119 high-quality sequences were obtained from the 36 samples, with an average sequence length of 290.68 bp. After quality filtering and denoising, 5,671 ASVs were generated. Taxonomic annotation assigned these ASVs to 18 phyla, 54 classes, 132 orders, 307 families, 594 genera, and 909 species.

Three sympatric snail species and composition of soil fungal communities

Fungal community composition was characterized at the phylum and genus levels (Fig. 4a). At the phylum level, Ascomycota dominated all samples. *A. ravida*, *R. decollata*, and Soil showed high relative abundances of Ascomycota (69.3–84.2%), whereas *E. aculus* had the lowest (41.5%). Basidiomycota was the second most abundant phylum, with higher proportions in *A. ravida* and *R. decollata* than in *E. aculus* and Soil. At the genus level, the dominant genera differed among groups. In *A. ravida*, *Blumeria* (27.4%), *Colletotrichum* (8.3%), and *Ganoderma* (7.7%) were dominant. *E. aculus* was characterized by *Alternaria* (4.8%), *Zygosaccharomyces* (2.4%), *Malassezia* (1.5%), and *Colletotrichum* (1.2%) being the most prevalent. In *R. decollata*, *Malassezia* (10.1%) was the dominant genus. Soil samples were characterized by *Kazachstania* (4.8%), *Ustilaginoidea* (4.1%), and *Aspergillus* (3.1%).

A Venn diagram further illustrated the distribution of shared and unique fungal genera among the four groups (Fig. 4b). *R. decollata* harbored 245 unique genera, the highest among the four groups, whereas *E. aculus* harbored only 9. Thirty-five fungal genera were shared among all four groups.

Diversity and compositional differentiation of fungal communities

Alpha diversity varied among groups (Fig. 4c). Chao1 and Shannon indices revealed that Soil harbored the richest and most diverse fungal community. In contrast, *E. aculus* exhibited the lowest fungal richness and diversity across both metrics. Furthermore, *R. decollata* showed substantial inter-individual variation in both Chao1 and Shannon values.

Weighted UniFrac-based PCoA and Bray-Curtis-based NMDS produced broadly consistent Beta diversity patterns (Fig. 4d). Soil samples were clearly separated from all snail gut samples, while *R. decollata* occupied a distinct region of the ordination space relative to *A. ravida* and *E. aculus*. *R. decollata* and *A. ravida* showed partial overlap but were not completely separated. PERMANOVA indicated significant differences among the four groups (PCoA: $F = 4.96$, $R^2 = 0.32$, $P = 0.001$; NMDS: $F = 6.33$, $R^2 = 0.37$, $P = 0.001$).

LEfSe analysis (LDA > 3.5) identified group-specific fungal biomarkers (Fig. 4e). *R. decollata* showed a strong enrichment of *Malassezia* (LDA > 4.5), along with Fungi (incertae sedis), *Fusarium*, and *Cladosporium*. *A. ravida* was characterized by the enrichment of *Ganoderma*, *Rhizopus*, and *Starmerella*. *E. aculus* was enriched in *Zygosaccharomyces* and *Saccharomycetales* (incertae sedis). The Soil group was enriched in *Kazachstania*, *Ustilaginoidea*, and *Aspergillus*.

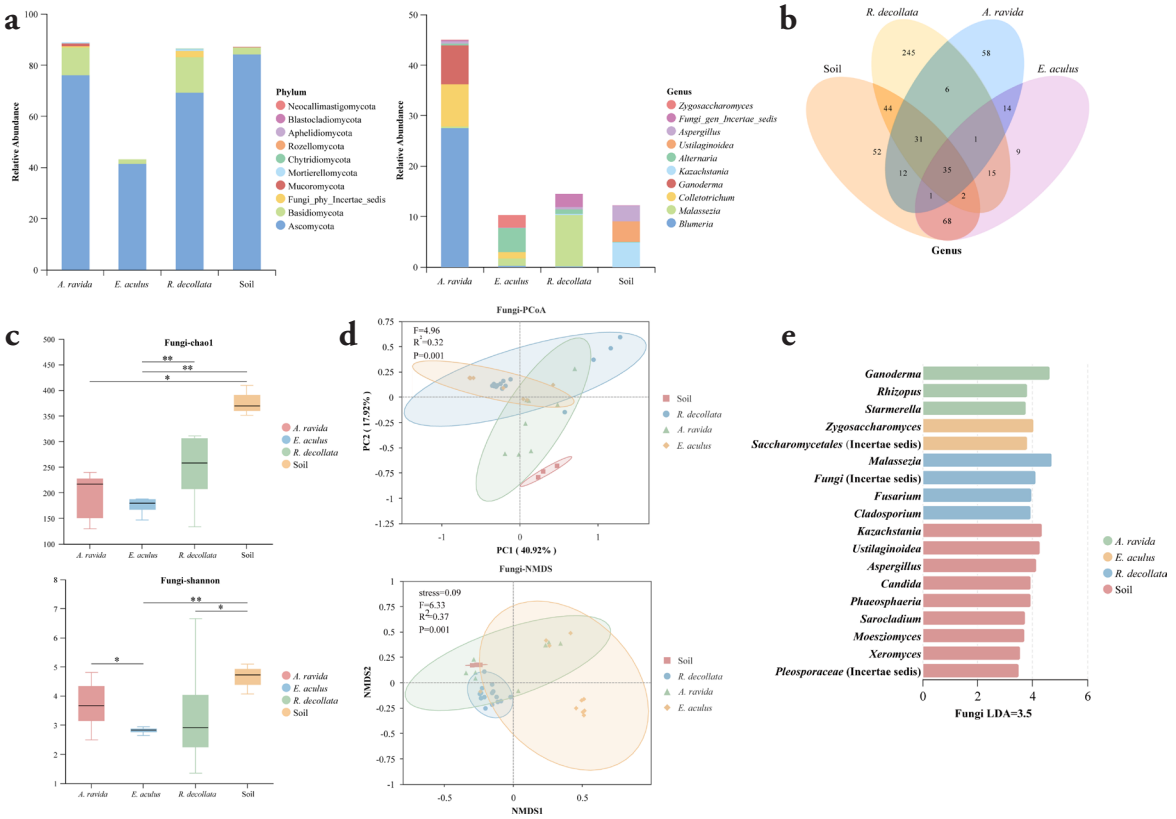

Figure 4. Fungal community composition and diversity of three sympatric snail species and associated soil. **a.** Relative abundance of dominant fungal taxa at the phylum (left) and genus (right) levels in the gut mycobiota of *Rumina decollata*, *Acusta ravida*, *Euphaedusa aculus*, and sympatric soil; **b.** Venn diagram showing the numbers of shared and unique fungal genera among the four groups; **c.** Alpha diversity of fungal communities based on the Chao1 richness and Shannon diversity indices. $*p \leq 0.05$, $**p \leq 0.01$; **d.** Beta diversity of fungal communities based on weighted UniFrac principal coordinate analysis (PCoA, upper side) and Bray-Curtis non-metric multidimensional scaling (NMDS, lower side); **e.** LEfSe analysis (LDA > 3.5) showing fungal taxa significantly enriched in each group.

Cross-domain bacterial–fungal association patterns

Cross-kingdom co-occurrence analysis revealed a modular organization of bacterial and fungal taxa across the four groups (Fig. 5a). Taxa predominantly associated with *R. decollata* were mainly clustered within connected sub-networks and were largely separated from the interconnected assemblage formed by the two native snail species and the soil environment. The integrated network comprised 63 nodes (49 bacterial and 14 fungal) and 273 edges, of which 96.7% (264 edges) represented positive correlations and 25.3% (69 edges) corresponded to cross-domain interactions. Within the *R. decollata* network, 157 nodes (116 bacterial and 41 fungal) were connected by 874 edges and organized into seven distinct modules (Fig. 5b). Positive correlations remained dominant (93.14%, 814 edges), whereas cross-domain interactions accounted for 18.2% (159 edges) of all edges. Several bacterial genera, including *Staphylococcus*, *Veillonella*, *Rothia*, and *Streptococcus*, together with the fungal genera *Malassezia* and *Aspergillus*, occupied highly connected positions within the network. Despite the extensive associations detected in the co-occurrence networks, Procrustes analysis revealed no significant concordance between bacterial and fungal community compositions (Suppl. material 1: fig. S1). Compared with the integrated network, the *R. decollata* network contained more nodes and interactions and exhibited greater topological complexity, including a higher average degree and a larger number of modules (Suppl. material 1: table S10).

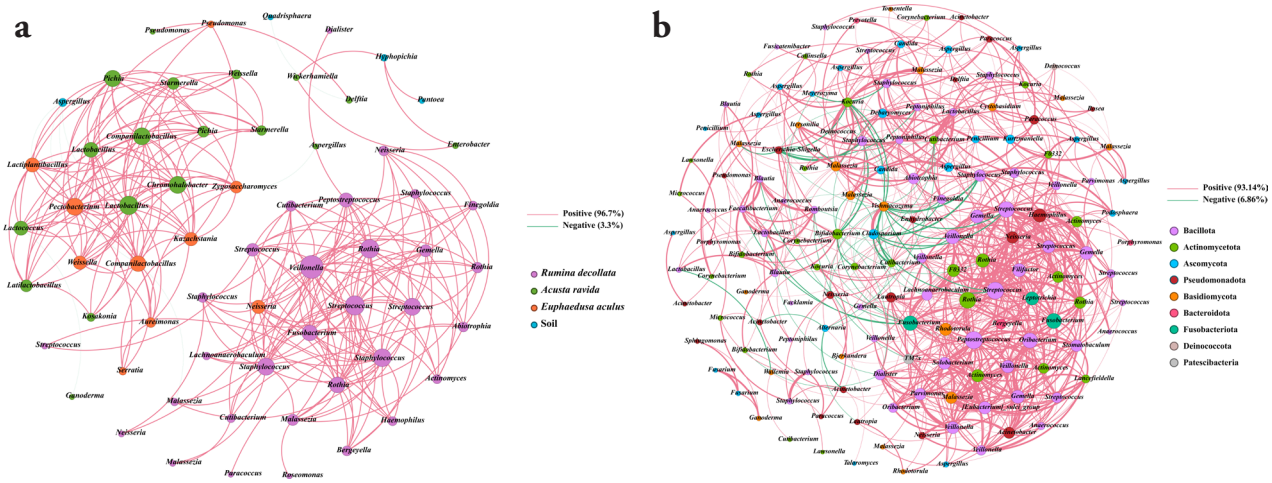

Figure 5. Cross-domain bacterial-fungal co-occurrence networks. **a.** Integrated bacterial–fungal co-occurrence network constructed using all samples; **b.** Cross-domain co-occurrence network constructed from the gut microbiome of *Rumina decollata*. Nodes represent bacteria or fungi and are colored according to taxonomic affiliation. Edges represent significant Spearman correlations after false discovery rate (FDR) correction ($P < 0.05$), with positive and negative associations indicated by different edge colors. Network modules were identified using the Louvain community detection algorithm.

Discussion

Habitat associated variation in gut microbial functional profiles

Despite belonging to the same host species, the gut microbiome of *R. decollata* exhibited pronounced habitat-specific functional differentiation across three habitats. This pattern indicates that gut microbial functional profiles varied among habitats and may be associated with differences in environmental conditions. Such functional plasticity may be relevant to the ecological persistence of *R. decollata* in different environments (Lozupone et al. 2012; Zhang et al. 2023). However, habitat differentiation was more pronounced for KEGG pathways than for the overall CAZy profile. The KEGG level 3 functional profile showed significant differentiation among different habitats, while the inter-group differences in the overall CAZy spectrum did not reach a statistically significant level. This contrast suggests that the broad functional framework of the gut microbiome remained relatively conserved, whereas habitat-associated variation was more evident in specific metabolic pathways.

At the KEGG pathway level, gut microbiomes from the more anthropogenically disturbed campus habitat (NF) exhibited a higher representation of pathways involved in environmental sensing and energy acquisition, including the two-component system (ko02020) and oxidative phosphorylation (ko00190), together with membrane transport functions such as ATP-binding cassette (ABC) transporters (Kanehisa and Goto 2000). Habitats subjected to stronger anthropogenic disturbance typically contain a broader diversity of anthropogenic organic inputs and environmental contaminants (Grimm et al. 2008). The enrichment of membrane transport systems and xenobiotic degradation pathways observed here is therefore consistent with an increased capacity of the gut microbiome to exploit heterogeneous resources and may be associated with differences in the types of environmental resources and chemical compounds encountered across habitats (Lyu et al. 2022; Makwarela et al. 2025). The higher abundance of xenobiotic degradation pathways in the campus habitat, including benzoate degradation (ko00362), may further reflect habitat-associated differences in environmental exposure.

At the CAZy level, while the macro-level enzyme profiles did not exhibit pronounced group-level differentiation, LEfSe analysis revealed habitat-associated differences in specific CAZy families. In the FS habitat, the gut microbiome was significantly enriched in chitinases (GH18) and chitin-binding modules (CBM14), along with α-amylases (GH13) and debranching enzymes (GH133), which are associated with the degradation of starch and α-glucan substrates, respectively, together with GH18 chitinases and the chitin-binding module CBM14, which contribute to the processing and binding of chitin-containing substrates. In terrestrial ecosystems, chitin can originate from arthropod exoskeletons, fungal cell walls, and other environmental sources (Beier and Bertilsson 2013). These enrichments therefore indicate increased microbial potential for processing starch-, α-glucan-, and chitin-containing substrates in the FS habitat. However, this enrichment does not directly establish the specific dietary sources of *R. decollata*. In contrast, the campus habitat (NF) showed enrichment of α-galactosidases (GH34), suggesting habitat-associated differences in the microbial capacity to process α-galactoside-containing carbohydrates. The NF habitat also showed enrichment of glycogen phosphorylases (GT35) and glycosyltransferases (GT2), indicating differences in the microbial potential for glycogen metabolism and polysaccharide biosynthesis under different habitat conditions (Wardman et al. 2022). Thus, the observed habitat-associated functional differentiation was characterized by enrichment of specific CAZy families while maintaining a broadly conserved carbohydrate metabolic repertoire. However, because environmental contaminants and other environmental variables were not directly measured, the specific factors underlying this functional differentiation cannot be determined.

Consistent with the KEGG results, the CARD and VFDB analyses further revealed habitat-associated differences in antibiotic resistance genes and virulence-associated functions. Artificial environments are widely recognized as important reservoirs of antimicrobial resistance, where anthropogenic activities increase the environmental abundance of resistance determinants (Martínez 2008; Forsberg et al. 2012). The higher abundance of individual ARGs observed in anthropogenically influenced habitats may therefore reflect differences in environmental exposure rather than active host adaptation, although this interpretation cannot be directly evaluated with the present data (Zhu et al. 2013). Therefore, these findings suggest that habitat-associated variation in specific microbial functions, together with the overall stability of the gut microbiome, may be relevant to the ecological persistence of *R. decollata* across heterogeneous habitats.

Host-associated differentiation of gut microbial communities

In contrast to the functional variation revealed by metagenomic analyses, the 16S rRNA gene and ITS datasets demonstrated pronounced taxonomic differentiation among the gut microbiomes of *R. decollata*, the two sympatric native snail species, and the surrounding soil. Both bacterial and fungal communities were clearly separated by host species, whereas soil samples formed an independent cluster, indicating host associated differentiation in gut microbial community composition. Similar host-associated patterns have been widely reported across animal microbiomes, where host physiology, gut physicochemical conditions, and immune regulation are considered important factors in shaping gut microbial communities (Ley et al. 2008; Colston and Jackson 2016).

Taxonomic composition further supported this pattern. LEfSe analysis identified several bacterial taxa, including *Cutibacterium*, *Corynebacterium*, and *Staphylococcus*, together with the fungal genus *Malassezia*, as characteristic members of the gut microbiome of *R. decollata*. These microorganisms have previously been reported from terrestrial environments and host-associated microbiomes, suggesting that they may occur in host-associated niches rather than representing transient environmental contaminants (Cardoso et al. 2012; Engel and Moran 2013; Amend 2014). Their consistent enrichment in *R. decollata* is consistent with a host-associated microbial assemblage despite continuous exposure to diverse environmental microorganisms.

In addition, although *R. decollata* harbored a distinct gut microbiota from the surrounding soil microbiota, its bacterial community partially overlapped with that of the sympatric native snail *A. ravida*. This pattern suggests that gut microbial assembly in *R. decollata* is not fully explained by environmental microbial availability, but may also reflect convergence associated with shared ecological conditions or resource utilization strategies. Previous ecological studies have described *R. decollata* as a dietary generalist capable of consuming plant material, detritus, fungi, and animal-derived resources, and the native snails examined here are considered predominantly herbivorous or detritivorous (Radwan and Gad 2021; Xu et al. 2024). Such differences in dietary resource utilization may expose hosts to distinct microbial source pools and contribute to differences in the metabolic potential of their gut microbiomes (Muegge et al. 2011; Bolnick et al. 2014). This interpretation is also consistent with the habitat-specific enrichment of carbohydrate-active enzyme families observed in the metagenomic analysis, suggesting that taxonomic differentiation and functional specialization may be associated with ecological resource utilization in *R. decollata*. Rather than indicating complete ecological isolation, these differences are consistent with potential ecological differentiation between *R. decollata* and sympatric native snail species and may provide a perspective rooted in the microbiome on their coexistence.

Cross-kingdom network decoupling and co-occurrence associations

Although bacterial and fungal communities constitute an integrated gut microbiome, they did not exhibit significant concordance at the whole-community level. Procrustes analysis revealed no significant association between bacterial and fungal community structures ($M^2 = 0.94$, $P = 0.226$), indicating that the assembly of these two microbial kingdoms was largely independent. This finding suggests that bacterial and fungal communities may respond differently to host-associated processes and environmental variation and may therefore be governed, at least in part, by distinct ecological processes (Coyte et al. 2015; de Vries et al. 2018).

In contrast to the lack of concordance at the community level, cross-domain co-occurrence networks revealed extensive positive associations between bacterial and fungal taxa, with more than 93% of significant correlations being positive. These associations indicate that bacterial and fungal taxa exhibited coordinated patterns of occurrence across samples, but their biological basis cannot be inferred from correlation-based analyses alone. Therefore, the observed positive associations are interpreted here as co-occurrence patterns rather than evidence of ecological interactions or functional cooperation (Faust and Raes 2012; Weiss et al. 2016).

These results reveal a hierarchical organization of the gut microbiome in *R. decollata*, characterized by decoupling at the macroscale and joint occurrence asso-

ciations at the microscale. At the community level, bacterial and fungal assemblages appear to be structured independently in association with host-related and environmental factors. However, these associations may be influenced by local environmental conditions or other ecological factors, although their underlying mechanisms remain unclear. Such differences between community composition and co-occurrence patterns may reflect different levels of organization within microbial communities, although the ecological significance of these associations requires further investigation (Coyte et al. 2015; Moya and Ferrer 2016). This hierarchical organization may therefore be relevant to the ecological persistence of *R. decollata* across different habitats. Based on these observations, we propose a conceptual framework in which habitat-associated variation is primarily reflected in microbial functional potential, whereas host-associated differentiation is reflected in taxonomic composition. Local associations between bacterial and fungal taxa further reveal patterns of co-occurrence, which may be relevant to the ecological persistence of *R. decollata* across heterogeneous habitats.

Several limitations should be considered when interpreting the habitat associated patterns observed in this study. The three sampling habitats represent distinct geographic locations, and environmental factors such as vegetation, soil properties, microclimate, and anthropogenic disturbance were not independently measured. Potential differences in host population structure were also not assessed. Therefore, the observed differences in microbial composition and functional potential cannot be attributed to any specific environmental factor, and the effects of environmental variables cannot be disentangled from geographic location. In particular, the enrichment of xenobiotic degradation functions in the NF habitat should not be interpreted as direct evidence of pesticide exposure or microbial adaptation to chemical pollution. Future studies incorporating environmental measurements and replicated sampling across locations will be necessary to identify the environmental drivers of gut microbiome variation in *R. decollata*.

In addition, because a species-specific reference genome for *R. decollata* was unavailable, host read removal relied on the available *A. fulica* reference genome, and residual host derived sequences cannot be completely excluded. We therefore implemented subsequent conservative processing measures based on the Micro_NR database to minimize potential confounding effects on downstream functional analyses.

Conclusions

This study reveals pronounced variation in the gut microbiome of the alien snail *R. decollata* across heterogeneous habitats. Habitat variation was primarily reflected by shifts in microbial functional potential rather than taxonomic composition, indicating that the gut microbiome exhibits functional variation associated with environmental heterogeneity. In contrast, gut bacterial and fungal communities differed among host species and were distinct from surrounding soil, suggesting that host-associated processes contribute to microbiome assembly. Together, these findings indicate that variation in microbial functional potential is associated with habitat heterogeneity and is consistent with potential ecological differentiation that may contribute to coexistence between *R. decollata* and sympatric native snails. Antibiotic resistance genes and virulence-associated functions were detected in the gut microbiome, indicating the presence of potential antibiotic resistance and traits linked to virulence that warrant further investigation.

References

Alcock BP, Raphenya AR, Lau TTY, Tsang KK, Bouchard M, Edalatmand A, Huynh W, Nguyen AV, Cheng AA, Liu S, Min SY, Miroshnichenko A, Tran HK, Werfalli RE, Nasir JA, Oloni M, Speicher DJ, Florescu A, Singh B, Faltyn M, McArthur AG (2020) CARD 2020: Antibiotic resistome surveillance with the comprehensive antibiotic resistance database. Nucleic Acids Research 48(D1): D517–D525. https://doi.org/10.1093/nar/gkz935

Amend A (2014) From dandruff to deep-sea vents: *Malassezia*-like fungi are ecologically hyper-diverse. PLOS Pathogens 10(8): e1004277. https://doi.org/10.1371/journal.ppat.1004277

Beier S, Bertilsson S (2013) Bacterial chitin degradation-mechanisms and ecophysiological strategies. Frontiers in Microbiology 4: e149. https://doi.org/10.3389/fmicb.2013.00149

Blackburn TM, Pyšek P, Bacher S, Carlton JT, Duncan RP, Jarošík V, Wilson JR, Richardson DM (2011) A proposed unified framework for biological invasions. Trends in Ecology & Evolution 26(7): 333–339. https://doi.org/10.1016/j.tree.2011.03.023

Bolnick DI, Snowberg LK, Hirsch PE, Lauber CL, Org E, Parks B, Lusis AJ, Knight R, Caporaso JG, Svanbäck R (2014) Individual diet has sex-dependent effects on vertebrate gut microbiota. Nature Communications 5: e4500. https://doi.org/10.1038/ncomms5500

Bolyen E, Rideout JR, Dillon MR, Bokulich NA, Abnet CC, Al-Ghalith GA, Alexander H, Alm EJ, Arumugam M, Asnicar F, Bai Y, Bisanz JE, Bittinger K, Brejnrod A, Brislawn CJ, Brown CT, Callahan BJ, Caraballo-Rodríguez AM, Chase J, Cope EK, Caporaso JG (2019) Reproducible, interactive, scalable and extensible microbiome data science using QIIME 2. Nature Biotechnology 37(8): 852–857. https://doi.org/10.1038/s41587-019-0209-9

Buchfink B, Xie C, Huson DH (2015) Fast and sensitive protein alignment using DIAMOND. Nature Methods 12(1): 59–60. https://doi.org/10.1038/nmeth.3176

Buchfink B, Reuter K, Drost HG (2021) Sensitive protein alignments at tree-of-life scale using DIAMOND. Nature Methods 18: 366–368. https://doi.org/10.1038/s41592-021-01101-x

Callahan BJ, McMurdie PJ, Rosen MJ, Han AW, Johnson AJ, Holmes SP (2016) DADA2: High-resolution sample inference from Illumina amplicon data. Nature Methods 13(7): 581–583. https://doi.org/10.1038/nmeth.3869

Caporaso JG, Lauber CL, Walters WA, Berg-Lyons D, Lozupone CA, Turnbaugh PJ, Fierer N, Knight R (2011) Global patterns of 16S rRNA diversity at a depth of millions of sequences per sample. Proceedings of the National Academy of Sciences of the United States of America 108 Suppl 1: 4516–4522. https://doi.org/10.1073/pnas.1000080107

Cardoso AM, Cavalcante JJ, Cantão ME, Thompson CE, Flatschart RB, Glogauer A, Scapin SM, Sade YB, Beltrão PJ, Gerber AL, Martins OB, Garcia ES, de Souza W, Vasconcelos AT (2012) Metagenomic analysis of the microbiota from the crop of an invasive snail reveals a rich reservoir of novel genes. PLOS ONE 7(11): e48505. https://doi.org/10.1371/journal.pone.0048505

Cardoso AM, Cavalcante JJ, Vieira RP, Lima JL, Grieco MA, Clementino MM, Vasconcelos AT, Garcia ES, de Souza W, Albano RM, Martins OB (2012) Gut bacterial communities in the giant land snail *Achatina fulica* and their modification by sugarcane-based diet. PLOS ONE 7(3): e33440. https://doi.org/10.1371/journal.pone.0033440

Chen S, Zhou Y, Chen Y, Gu J (2018) fastp: An ultra-fast all-in-one FASTQ preprocessor. Bioinformatics 34(17): i884–i890. https://doi.org/10.1093/bioinformatics/bty560

Colston TJ, Jackson CR (2016) Microbiome evolution along divergent branches of the vertebrate tree of life: What is known and unknown. Molecular Ecology 25(16): 3776–3800. https://doi.org/10.1111/mec.13730

Cowie RH (2001) Invertebrate invasions on Pacific islands and the replacement of unique native faunas: A synthesis of the land and freshwater snails* Contribution no. 2001-001 of

Bishop Museum's Pacific Biological Survey. Biological Invasions 3(2): 119–136. https://doi.org/10.1023/A:1014529019000

Coyte KZ, Schluter J, Foster KR (2015) The ecology of the microbiome: Networks, competition, and stability. Science 350(6261): 663–666. https://doi.org/10.1126/science.aad2602

de Vries FT, Griffiths RI, Bailey M, Craig H, Girlanda M, Gweon HS, Hallin S, Kaisermann A, Keith AM, Kretzschmar M, Lemanceau P, Lumini E, Mason KE, Oliver A, Ostle N, Prosser JI, Thion C, Thomson B, Bardgett RD (2018) Soil bacterial networks are less stable under drought than fungal networks. Nature Communications 9(1): e3033. https://doi.org/10.1038/s41467-018-05516-7

Douglas AE (2015) Multiorganismal insects: diversity and function of resident microorganisms. Annual Review of Entomology 60: 17–34. https://doi.org/10.1146/annurev-ento-010814-020822

Engel P, Moran NA (2013) The gut microbiota of insects – diversity in structure and function. FEMS Microbiology Reviews 37(5): 699–735. https://doi.org/10.1111/1574-6976.12025

Faust K, Raes J (2012) Microbial interactions: from networks to models. Nature Reviews Microbiology 10(8): 538–550. https://doi.org/10.1038/nrmicro2832

Forsberg KJ, Reyes A, Wang B, Selleck EM, Sommer MOA, Dantas G (2012) The shared antibiotic resistome of soil bacteria and human pathogens. Science 337(6098): 1107–1111. https://doi.org/10.1126/science.1220761

Forslund K, Hildebrand F, Nielsen T, Falony G, Le Chatelier E, Sunagawa S, Prifti E, Vieira-Silva S, Gudmundsdottir V, Pedersen HK, Arumugam M, Kristiansen K, Voigt AY, Vestergaard H, Hercog R, Costea PI, Kultima JR, Li J, Jørgensen T, Levenez F, Pedersen O (2015) Disentangling type 2 diabetes and metformin treatment signatures in the human gut microbiota. Nature 528(7581): 262–266. https://doi.org/10.1038/nature15766

Fu L, Niu B, Zhu Z, Wu S, Li W (2012) CD-HIT: Accelerated for clustering the next-generation sequencing data. Bioinformatics 28(23): 3150–3152. https://doi.org/10.1093/bioinformatics/bts565

Grimm NB, Faeth SH, Golubiewski NE, Redman CL, Wu J, Bai X, Briggs JM (2008) Global change and the ecology of cities. Science 319(5864): 756–760. https://doi.org/10.1126/science.1150195

Guo Y, Zhang Y, Liu Q, Huang Y, Mao G, Yue Z, Abe EM, Li J, Wu Z, Li S, Zhou X, Hu W, Xiao N (2019) A chromosomal-level genome assembly for the giant African snail Achatina fulica. GigaScience 8(10): giz124. https://doi.org/10.1093/gigascience/giz124

Wardman JF, Bains RK, Rahfeld P, Withers SG (2022) Carbohydrate-active enzymes (CAZymes) in the gut microbiome. Nature Reviews Microbiology, 20(9): 542–556. https://doi.org/10.1038/s41579-022-00712-1 Hai C, Wang L, Wu D, Pei D, Yang Y, Liu X, Zhao Y, Bai C, Su G, Bao Z, Yang L, Li G (2025) Loss of *Myostatin* leads to low production of CH_4 by altering rumen microbiota and metabolome in cattle. International Journal of Biological Macromolecules 294: e139533. https://doi.org/10.1016/j.ijbiomac.2025.139533

Herlemann DP, Labrenz M, Jürgens K, Bertilsson S, Waniek JJ, Andersson AF (2011) Transitions in bacterial communities along the 2000 km salinity gradient of the Baltic Sea. The ISME Journal 5(10): 1571–1579. https://doi.org/10.1038/ismej.2011.41

Huson DH, Beier S, Flade I, Górska A, El-Hadidi M, Mitra S, Ruscheweyh HJ, Tappu R (2016) MEGAN Community Edition - Interactive Exploration and Analysis of Large-Scale Microbiome Sequencing Data. PLOS Computational Biology 12(6): e1004957. https://doi.org/10.1371/journal.pcbi.1004957

Kanehisa M, Goto S (2000) KEGG: Kyoto Encyclopedia of Genes and Genomes. Nucleic Acids Research 28(1): 27–30. https://doi.org/10.1093/nar/28.1.27

Kwong WK, Medina LA, Koch H, Sing KW, Soh EJY, Ascher JS, Jaffé R, Moran NA (2017) Dynamic microbiome evolution in social bees. Science Advances 3(3): e1600513. https://doi.org/10.1126/sciadv.1600513

Langmead B, Salzberg SL (2012) Fast gapped-read alignment with Bowtie 2. Nature Methods 9(4): 357–359. https://doi.org/10.1038/nmeth.1923

Lee PY, Costumbrado J, Hsu CY, Kim YH (2012) Agarose gel electrophoresis for the separation of DNA fragments. Journal of Visualized Experiments 62: e3923. https://doi.org/10.3791/3923

Ley RE, Hamady M, Lozupone C, Turnbaugh PJ, Ramey RR, Bircher JS, Schlegel ML, Tucker TA, Schrenzel MD, Knight R, Gordon JI (2008) Evolution of mammals and their gut microbes. Science 320(5883): 1647–1651. https://doi.org/10.1126/science.1155725

Li D, Liu CM, Luo R, Sadakane K, Lam TW (2015) MEGAHIT: An ultra-fast single-node solution for large and complex metagenomics assembly via succinct de Bruijn graph. Bioinformatics 31(10): 1674–1676. https://doi.org/10.1093/bioinformatics/btv033

Liu B, Zheng D, Jin Q, Chen L, Yang J (2019) VFDB 2019: A comparative pathogenomic platform with an interactive web interface. Nucleic Acids Research 47(D1): D687–D692. https://doi.org/10.1093/nar/gky1080

Lombard V, Golaconda Ramulu H, Drula E, Coutinho PM, Henrissat B (2014) The carbohydrate-active enzymes database (CAZy) in 2013. Nucleic Acids Research 42(Database issue): D490–D495. https://doi.org/10.1093/nar/gkt1178

Lozupone CA, Stombaugh JI, Gordon JI, Jansson JK, Knight R (2012) Diversity, stability and resilience of the human gut microbiota. Nature 489(7415): 220–230. https://doi.org/10.1038/nature11550

Lyu T, Zhu J, Yang X, Yang W, Zheng Z (2022) Responses of gut microbial community composition and function of the freshwater gastropod *Bellamya aeruginosa* to Cyanobacterial bloom. Frontiers in Microbiology 13: e906278. https://doi.org/10.3389/fmicb.2022.906278

Magoč T, Salzberg SL (2011) FLASH: Fast Length Adjustment of Short reads to improve genome assemblies. Bioinformatics 27(21): 2957–2963. https://doi.org/10.1093/bioinformatics/btr507

Makwarela TG, Seoraj-Pillai N, Nangammbi TC (2025) Exploring the molluscan microbiome: Diversity, function, and ecological implications. Biology 14(8): e1086. https://doi.org/10.3390/biology14081086

Martínez JL (2008) Antibiotics and antibiotic resistance genes in natural environments. Science 321(5887): 365–367. https://doi.org/10.1126/science.1159483

McFall-Ngai M, Hadfield MG, Bosch TC, Carey HV, Domazet-Lošo T, Douglas AE, Wernegreen JJ (2013) Animals in a bacterial world, a new imperative for the life sciences. Proceedings of the National Academy of Sciences of the United States of America 110(9): 3229–3236. https://doi.org/10.1073/pnas.1218525110

Moya A, Ferrer M (2016) Functional redundancy-induced stability of gut microbiota subjected to disturbance. Trends in Microbiology 24(5): 402–413. https://doi.org/10.1016/j.tim.2016.02.002

Muegge BD, Kuczynski J, Knights D, Clemente JC, González A, Fontana L, Henrissat B, Knight R, Gordon JI (2011) Diet drives convergence in gut microbiome functions across mammalian phylogeny and within humans. Science 332(6032): 970–974. https://doi.org/10.1126/science.1198719

Nakayama Y, Yamaguchi H, Einaga N, Esumi M (2016) Pitfalls of DNA quantification using dna-binding fluorescent dyes and suggested solutions. PLOS ONE 11(3): e0150528. https://doi.org/10.1371/journal.pone.0150528

Nilsson RH, Larsson KH, Taylor AFS, Bengtsson-Palme J, Jeppesen TS, Schigel D, Kennedy P, Picard K, Glöckner FO, Tedersoo L, Saar I, Kõljalg U, Abarenkov K (2019) The UNITE database for molecular identification of fungi: handling dark taxa and parallel taxonomic classifications. Nucleic Acids Research 47(D1): D259–D264. https://doi.org/10.1093/nar/gky1022

Pawar KD, Banskar S, Rane SD, Charan SS, Kulkarni GJ, Sawant SS, Ghate HV, Patole MS, Shouche YS (2012) Bacterial diversity in different regions of gastrointestinal tract of Giant African snail (*Achatina fulica*). MicrobiologyOpen 1(4): 415–426. https://doi.org/10.1002/mbo3.38

Pierce ML, Ward JE (2019) Gut microbiomes of the eastern oyster (*Crassostrea virginica*) and the blue mussel (*Mytilus edulis*): Temporal variation and the influence of marine aggregate-associated microbial communities. mSphere 4(6): e00730–19. https://doi.org/10.1128/msphere.00730-19

Pizá J, Spagnuoli JG, Dop NS, Cazzaniga NJ (2023) From the Mediterranean to Yungas and Patagonia. Dispersal of the non-native gastropod *Rumina decollata* in Argentina. Biologia 78(3): 865–871. https://doi.org/10.1007/s11756-022-01293-3

Quail MA, Smith M, Coupland P, Otto TD, Harris SR, Connor TR, Bertoni A, Swerdlow HP, Gu Y (2012) A tale of three next generation sequencing platforms: Comparison of Ion Torrent, Pacific Biosciences and Illumina MiSeq sequencers. BMC Genomics 13: e341. https://doi.org/10.1186/1471-2164-13-341

Quast C, Pruesse E, Yilmaz P, Gerken J, Schweer T, Yarza P, Peplies J, Glöckner FO (2013) The SILVA ribosomal RNA gene database project: Improved data processing and web-based tools. Nucleic Acids Research 41(Database issue): D590–D596. https://doi.org/10.1093/nar/gks1219

Quince C, Walker AW, Simpson JT, Loman NJ, Segata N (2017) Shotgun metagenomics, from sampling to analysis. Nature Biotechnology 35(9): 833–844. https://doi.org/10.1038/nbt.3935

Radwan MA, Gad AF (2021) Essential oils and their components as promising approach for gastropod mollusc control: A review. Journal of Plant Diseases and Protection 128(4): 923–949. https://doi.org/10.1007/s41348-021-00484-5

Richardson DM, Pyšek P (2012) Naturalization of introduced plants: Ecological drivers of biogeographical patterns. New Phytologist 196(2): 383–396. https://doi.org/10.1111/j.1469-8137.2012.04292.x

Santamaria B, Verbeken A, Haelewaters D (2023) Mycophagy: A global review of interactions between invertebrates and fungi. Journal of Fungi 9(2): e163. https://doi.org/10.3390/jof9020163

Toju H, Tanabe AS, Yamamoto S, Sato H (2012) High-coverage ITS primers for the DNA-based identification of ascomycetes and basidiomycetes in environmental samples. PLOS ONE 7(7): e40863. https://doi.org/10.1371/journal.pone.0040863

Vellend M (2010) Conceptual synthesis in community ecology. The Quarterly Review of Biology 85(2): 183–206. https://doi.org/10.1086/652373

Wang W, Zheng S, Sharshov K, Sun H, Yang F, Wang X, Li L, Xiao Z (2017) Metagenomic profiling of gut microbial communities in both wild and artificially reared Bar-headed goose (*Anser indicus*). MicrobiologyOpen 6(2): e00429. https://doi.org/10.1002/mbo3.429

Wang X, Li H, Yang Y, Wu Z, Wang Z, Li D, Xia W, Zou S, Liu Y, Wang F (2024) Geographic and environmental impacts on gut microbiome in Himalayan langurs (*Semnopithecus schistaceus*) and Xizang macaques (*Macaca mulatta vestita*). Frontiers in Microbiology 15: e1452101. https://doi.org/10.3389/fmicb.2024.1452101

Wardman JF, Bains RK, Rahfeld P, Withers SG (2022) Carbohydrate-active enzymes (CAZymes) in the gut microbiome. Nature Reviews Microbiology 20(9): 542–556. https://doi.org/10.1038/s41579-022-00712-1

Weiss S, Van Treuren W, Lozupone C, Faust K, Friedman J, Deng Y, Xia LC, Xu ZZ, Ursell L, Alm EJ, Birmingham A, Cram JA, Fuhrman JA, Raes J, Sun F, Zhou J, Knight R (2016) Correlation detection strategies in microbial data sets vary widely in sensitivity and precision. The ISME Journal 10(7): 1669–1681. https://doi.org/10.1038/ismej.2015.235

Winnepenninckx B, Backeljau T, De Wachter R (1993) Extraction of high molecular weight DNA from molluscs. Trends in Genetics 9(12): e407. https://doi.org/10.1016/0168-9525(93)90102-n

Xu W, Bai Y, Xu T, Chen Y, Wang J, Li T, Liu Z, Liu H, Ruan H (2024) Revealing potential mechanisms of native and non-native snail coexistence through fecal microbiomes and dietary compositions. Science of the Total Environment 957: e177774. https://doi.org/10.1016/j.scitotenv.2024.177774

Yun JH, Roh SW, Whon TW, Jung MJ, Kim MS, Park DS, Bae JW (2014) Insect gut bacterial diversity determined by environmental habitat, diet, developmental stage, and phylogeny of host. Applied and Environmental Microbiology 80(17): 5254–5264. https://doi.org/10.1128/AEM.01226-14

Zhang Y, Su JQ, Liao H, Breed MF, Yao H, Shangguan H, Li HZ, Sun X, Zhu YG (2023) Increasing antimicrobial resistance and potential human bacterial pathogens in an invasive land snail

driven by urbanization. Environmental Science & Technology 57(18): 7273–7284. https://doi.org/10.1021/acs.est.3c01233

Zhu W, Lomsadze A, Borodovsky M (2010) Ab initio gene identification in metagenomic sequences. Nucleic Acids Research 38(12): e132. https://doi.org/10.1093/nar/gkq275

Zhu YG, Johnson TA, Su JQ, Qiao M, Guo GX, Stedtfeld RD, Hashsham SA, Tiedje JM (2013) Diverse and abundant antibiotic resistance genes in Chinese swine farms. Proceedings of the National Academy of Sciences of the United States of America 110(9): 3435–3440. https://doi.org/10.1073/pnas.1222743110

Additional information

Conflict of interest

The authors have declared that no competing interests exist.

Ethical statement

This work was permitted Animal Ethics Committee of Nanjing Forestry University.

Artificial Intelligence (AI) use

The authors accept full responsibility for the content of the manuscript, including the disclosure of any use of AI.
No AI tools were used in the preparation of this manuscript.

Funding

No funding was reported.

Author contributions

Conception: HL. Sampling: YX, MG, YL. Experimentation: YX, MG. Bioinformatic analysis: YX, GZ. Writing – original draft: YX. Writing – review and editing: HL, YX, MG, GZ, YL. All authors have read and approved the final manuscript.

Author ORCIDs

Y. Xu https://orcid.org/0009-0005-4440-2110
M. Gao https://orcid.org/0009-0007-5302-9287
G. Zhang https://orcid.org/0009-0001-2096-2288
Y. Li https://orcid.org/0009-0004-9318-2663
H. Liu https://orcid.org/0000-0003-2081-5779

Data availability

The raw sequencing data generated in this study have been deposited in the NCBI (PRJNA1461374, PRJNA1494890, PRJNA1461886). All other data that support the findings of this study are available in the main text and supplementary materials.

Supplementary material 1

Supplementary information

Authors: Yang Xu, Ming Gao, Gaoji Zhang, Yingzhu Li, Hongyi Liu

Data type: docx

Explanation note: **table S1.** Summary statistics of metagenomic sequencing quality and de novo assembly of gut microbiomes from *Rumina decollata*. **table S2.** Taxonomic composition of the metagenomic gene catalogue across 18 *Rumina decollata* samples based on Micro_NR annotation. **table S3.** KEGG level 3 pathways shown in the heatmap and their functional classifications. **table S4.** Differentially enriched KEGG level 3 pathways identified by LEfSe analysis. **table S5.** Relative abundance of CAZy families across different habitats. **table S6.** Differentially abundant CAZy families identified by LEfSe analysis. **table S7.** Relative abundance of virulence factor categories identified by VFDB across different habitats. **table S8.** Differentially abundant VFDB virulence factors identified by LEfSe analysis. **table S9.** Relative abundance (%) of antibiotic resistance gene (ARG) categories across different habitats. Table S10. Topological properties of bacterial–fungal co-occurrence networks. **fig. S1.** Procrustes analysis of bacterial and fungal community compositions.

Copyright notice: This dataset is made available under the Open Database License (http://opendatacommons.org/licenses/odbl/1.0/). The Open Database License (ODbL) is a license agreement intended to allow users to freely share, modify, and use this Dataset while maintaining this same freedom for others, provided that the original source and author(s) are credited.

Link: https://doi.org/10.3897/neobiota.110.208923.suppl1